RESEARCH PAPER

Rapamycin affects early fracture healing in mice

JH Holstein[1,2], M Klein[1,2], P Garcia[1,2], T Histing[1,2], U Culemann[1], A Pizanis[1], MW Laschke[2], C Scheuer[2], C Meier[2], H Schorr[3], T Pohlemann[1] and MD Menger[2]

[1]Department of Trauma, Hand and Reconstructive Surgery, Homburg/Saar, Germany; [2]Institute for Clinical & Experimental Surgery, Homburg/Saar, Germany and [3]Department of Laboratory Medicine, University of Saarland, Homburg/Saar, Germany

Background and purpose: The immunosuppressive drug rapamycin (RAPA) prevents rejection in organ transplantation by inhibiting interleukin-2-stimulated T-cell division. Rapamycin has also been suggested to possess strong anti-angiogenic activities linked to a decrease in production of vascular endothelial growth factor (VEGF). Angiogenesis and VEGF are thought to play a crucial role in fracture healing and as osteoporotic and traumatic fractures are common complications in immunosuppressed, organ transplantation patients, we conducted this study to analyze the effect of rapamycin treatment on bone repair.

Experimental approach: We investigated the effect of rapamycin treatment on bone repair in a murine closed femur fracture model using radiological, histomorphometric, immunohistochemical, biomechanical and protein biochemical analyses.

Key results: X-ray analyses demonstrated that rapamycin treatment inhibits callus formation after two weeks of fracture healing. The radiologically observed lack of callus formation was confirmed by histomorphometric analyses, which revealed a significantly diminished callus size and a reduced amount of bone formation when compared with vehicle-treated controls. Biomechanical testing further demonstrated that rapamycin significantly reduces torsional stiffness of the callus. Interestingly, this effect was associated with decreased vessel formation; a diminished proliferation of osteoblasts, endothelial cells and periosteal cells; and a reduced VEGF expression in hypertrophic chondrocytes. After five weeks treatment, however, the negative impact of rapamycin on fracture healing was overcome.

Conclusions and implications: Thus, rapamycin initially delays fracture healing, most probably by inhibiting cell proliferation and neovascularization in the callus. These undesirable effects should be considered when rapamycin is administered to patients sustaining bone fractures.

British Journal of Pharmacology (2008) **154**, 1055–1062; doi:10.1038/bjp.2008.167; published online 5 May 2008

Introduction

Over the last 20 years organ transplantation has become an established treatment in a multitude of human conditions. Improved postoperative patient outcome has meant that the concomitant immunosuppression may impinge upon routine clinical practise. Osteoporotic and traumatic fractures are relatively common in transplant patients and the successful treatment is important for patient outcome and quality of life (Navasa *et al.*, 1996).

The long-term prognosis of transplant patients is highly dependent on an appropriate immunosuppression. However, several studies have demonstrated negative influences of rapamycin (Sirolimus) and other immunosuppressive drugs on bone metabolism and development (Romero *et al.*, 1995; Stempfle *et al.*, 2002; Compston, 2003; Vossen *et al.*, 2005; Alvarez-Garcia *et al.*, 2007). Rapamycin is an immunosuppressive drug, which today is widely used to prevent transplant rejection. Immunosuppression is achieved by the inhibition of interleukin-2-stimulated T-cell division (Wiederrecht *et al.*, 1995). Forming a complex with the FK-binding protein-12 rapamycin blocks the mammalian target of rapamycin (mTOR), which is a key controller of multiple mitogenic signaling pathways (Schmelzle and Hall, 2000). Interestingly, beside its role as an immunosuppressive drug,

rapamycin has also been suggested to inhibit tumour growth and metastasis (Guba *et al.*, 2002), which is in contrast to the most widely recognized immunosuppressive drug cyclosporin, which is known to promote rather than to inhibit the development of cancer (Kauffman *et al.*, 2006). In fact, rapamycin has been shown to prevent tumour growth by inhibiting the process of angiogenesis and vascularization. This specific effect seems to be linked to a reduced production of the vascular endothelial growth factor (VEGF) and consequently to a decrease of VEGF-induced endothelial cell signaling after rapamycin treatment (Guba *et al.*, 2002).

Beside tumour cells, pancreatic island cells and epidermal cells show a significantly diminished expression of VEGF after rapamycin treatment (Cross *et al.*, 2007; Schaffer *et al.*, 2007). Interestingly, Alvarez-Garcia *et al.* (2007) identified a critical reduction of VEGF expression in hypertrophic chondrocytes within the growth plate of young rapamycin-treated rats, associated with severe skeletal growth retardations.

VEGF is also known to be one of the key molecules promoting angiogenesis during fracture healing (Ferguson *et al.*, 1999). Additionally, VEGF is expressed in terminally differentiating chondrocytes during bone repair, indicating an important role of VEGF in the degradation of hypertrophic cartilage matrix (Neufeld *et al.*, 1999). Recent studies further reported an improved osteogenesis and angiogenesis in large segmental bone defects due to VEGF treatment (Geiger *et al.*, 2005). However, there is no information on whether rapamycin affects fracture healing.

Because of the increased frequency of rapamycin treatment in patients after organ transplantation, it follows that the number of patients sustaining bone fractures under rapamycin treatment will also grow. Hence, we decided to investigate the effects of rapamycin treatment on the process of experimental fracture healing in mice.

Methods

Experimental groups

All animal procedures were performed according to the National Institute of Health guidelines for the use of experimental animals and were approved by the German legislation on the protection of animals.

For the present study, 38 SKH1-Hr mice (30–40 g body weight) were treated by a daily intraperitoneal (i.p.) injection of rapamycin ($1.5\,mg\,kg^{-1}\,d^{-1}$) from the day of fracture until they were killed. Two or 5 weeks after fracture, animals were killed and bone healing was analyzed using radiological ($n = 16$ each at 2 and 5 weeks), biomechanical ($n = 8$ each), histomorphometric ($n = 8$ each), and immunohistochemical ($n = 4$ at 2 weeks) methods. At 2 weeks additional animals were studied to sample tissue for western blot ($n = 3$) and ELISA analyses ($n = 3$). Vehicle-treated mice, served as controls. In these animals, bone healing was analyzed using radiological ($n = 16$ at 2 weeks and $n = 15$ at 5 weeks), biomechanical ($n = 8$ each), histomorphometric ($n = 8$ at 2 weeks and $n = 7$ at 5 weeks) and immunohistochemical ($n = 4$ at 2 weeks) methods. At 2 weeks additional control animals

were studied to sample tissue for western blot ($n = 3$) and ELISA analyses ($n = 3$).

Surgical procedure

Mice were anesthetized by an i.p. injection of xylazine ($25\,mg\,kg^{-1}$) and ketamine ($75\,mg\,kg^{-1}$). The right femur of each animal was fractured by a 3-point bending device and stabilized using a locking nail as described previously (Holstein *et al.*, 2007a). Fracture configuration, that is, a closed midshaft fracture type A2-A3 according to AO classification (Müller *et al.*, 1990), and implant position were documented by X-rays (Inside IP-21 high resolution dental films, Kodak, Rochester, NY, USA).

Rapamycin serum concentration

Based on recommendations for the clinical use of rapamycin, rapamycin serum concentration was determined by means of liquid chromatography-tandem mass spectrometric (LC-MS/MS) analysis after 2 weeks of daily application (MacDonald *et al.*, 2000; Wallemacq *et al.*, 2003).

Radiological analysis

X-rays of the healed femora were digitized. Using the Cap Image Analysis System (Zeintl, Heidelberg, Germany) the diameter of the callus in relation to the diameter of the femur at the fracture site was calculated.

Biomechanical analysis

After death, both the right and the left femora were prepared for torsional testing as reported previously (Holstein *et al.*, 2007a). The testing device consists of one fixed and one pivoted axis. The proximal and distal ends of the femur are embedded in 8-mm-diameter steal moulds filled with PMMA. At the free axis a predened torque is applied. The rotation angle is measured using a laser pointer and a circular disc. Parameters of the fractured femora are given in percent of the corresponding unfractured contralateral femora:
- Peak torque at failure (%)
- Peak rotation angle at failure (%)
- Torsional stiffness (%)

Histomorphometric analysis

The healed femora were fixed in 4% phosphate-buffered formalin for 24 h, decalcified in 10% EDTA solution for 5 weeks, and embedded in paraffin.

Longitudinal sections of 5 μm thickness were stained according to the trichrome method. The central slide of each specimen was analyzed at a magnification of 1.25 × (Olympus BX60 Microscope, Olympus, Tokyo, Japan; Zeiss Axio Cam and Axio Vision 3.1, Carl Zeiss, Oberkochen, Germany; ImageJ Analysis System, NIH, Bethesda, MD, USA). In adherence to the recommendations of the American Society of Bone and Mineral Research (ASBMR) (Parfitt *et al.*, 1987) the following histomorphometric parameters were calculated:

- Total callus area in relation to femoral bone diameter at the fracture gap [Cl.Ar B.Dm^{-1} (mm^2 mm^{-1})]
- Bone callus area (mineralized bone, osteoid and bone marrow) in relation to total callus area [B.Cl.Ar Cl.Ar^{-1} (%)]
- Cartilaginous callus area in relation to total callus area [Cg.Cl.Ar Cl.Ar^{-1} (%)]
- Fibrous callus area in relation to total callus area [Fb.Cl.Ar Cl.Ar^{-1} (%)]

Immunohistochemical analysis
Immunohistochemical staining for proliferating cell nuclear antigen (PCNA) and VEGF was used. Tissue sections were deparaffinized in xylene and rehydrated in a descending, graded series of alcohol. Endogenous peroxidase was blocked by 3% H$_2$O$_2$ (10 min). Antigen retrieval was achieved by microwaving (10 min; 700 W) specimens in citrate buffer (pH 6.0) or EDTA buffer (pH 9.0). After blocking unspecific binding sites with PBS and goat normal serum (30 min; room temperature), sections were incubated overnight with mouse monoclonal anti-PCNA (1:50 PBS; PC10, Dako Cytomation, Glostrup, Denmark) or with mouse monoclonal anti-VEGF (1:50 PBS; M7273, Dako Cytomation) antibodies at room temperature. Peroxidase-conjugated goat anti-mouse antibodies (1:100; Amersham Biosciences, Buckinghamshire, UK) were used as secondary antibodies (incubation for 1 h at room temperature). DAB (Dako Cytomation) served as the chromogen and Mayer's hemalum as the counterstain.

PCNA and VEGF expression were additionally quantified. PCNA-positive staining was found in periosteal cells, endothelial cells and osteoblasts, VEGF-positive staining in hypertrophic chondrocytes. The number of positive cells was quantitated and expressed as a percentage of the total number of the accordant cell type.

Vascular density analysis
To assess angiogenesis, area density of vessel profiles was analyzed at the transition between hypertrophic cartilage and woven bone using the PCNA-stained sections.

Western blot analysis
To evaluate cell proliferation within the callus, western blot analysis for PCNA was performed after 2 weeks of fracture healing. In addition, VEGF protein expression was also evaluated by western blot analysis.

Before death, mice were anesthetized to remove soft tissue cover around the diaphyseal part of the femora. Subsequently, all macroscopically visible aspects of the callus were resected and frozen in nitrogen. Accordingly, callus samples comprised of cartilage, bone, fibrous tissue, bone marrow and periosteum.

For extraction of the whole-protein fraction, frozen tissue samples were homogenized in lysis buffer, incubated for 30 min on ice and centrifuged for additional 30 min at 16 000 g. The supernatant was saved as whole-protein fraction, and protein concentrations were determined using the Lowry assay with BSA as standard. Subsequently, 60 µg protein per lane were separated discontinuously on 10% sodium dodecylsulphate polyacrylamide gels and transferred to a polyvinyldifluoride membrane (BioRad, Munich, Germany). After blockade of non-specific binding sites, membranes were incubated for 2 h with mouse monoclonal anti-PCNA (Dako Cytomation) or mouse monoclonal anti-VEGF antibodies (Santa Cruz Biotechnology, Santa Cruz, CA, USA). Protein expression was visualized by means of luminal-enhanced chemiluminescence and exposure of membranes to blue light-sensitive autoradiography film (Hyperfilm ECL; Amersham Biosciences). Signals were densitometrically assessed (Geldoc, Quantity one software; BioRad, Hercules, CA, USA) and normalized to β-actin signals (mouse anti-β-actin; Sigma, Taufkirchen, Germany) to correct unequal loading.

ELISA analysis
To quantify PCNA and VEGF expression additional callus samples were analyzed by ELISA methods. Tissue samples were obtained similarly as those obtained for western blot analysis. The whole-protein fraction was extracted as described above. Protein concentrations were determined using the PCNA enzyme immunoassay kit QIA59 (EMD Chemicals, Darmstadt, Germany) and the VEGF enzyme immunoassay kit DY493 (R & D Systems, Minneapolis, MN, USA).

Statistics
All data are given as mean ± s.d. After proving normal distribution and equal variance, comparison between the experimental groups was performed by one-way ANOVA followed by Student–Newman–Keuls test, which includes a correction of the α-error to compensate for multiple comparisons. Statistics were performed using the SigmaStat software package (Jandel, San Rafael, CA, USA). A P-value <0.05 was considered to indicate significant differences.

Results

Rapamycin serum concentration
After 2 weeks of daily rapamycin treatment serum concentrations were found in the therapeutic range when used for immunosuppression after organ transplantation (17.4 ± 5.5 ng mL^{-1}).

Radiological analysis
Two weeks post-fracture radiological analysis showed an almost complete lack of callus formation in the rapamycin-treated animals. Accordingly, the diameter of the callus was significantly decreased when compared with that of vehicle-treated controls. However, at 5 weeks rapamycin-treated animals revealed an increase in callus diameter, whereas the size of the callus in vehicle-treated controls was found decreased at this late time point. Thus, the difference in callus formation between the two groups observed at 2 weeks had disappeared by 5 weeks (Figure 1).
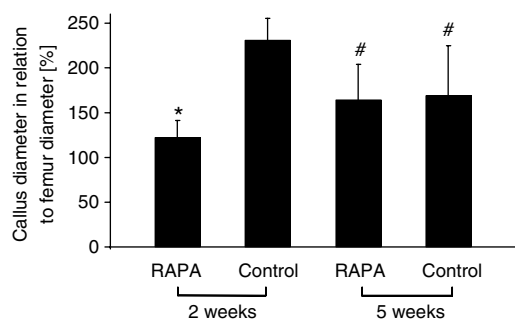
Biomechanical analysis
At 2 weeks post-fracture, peak torque at failure did not differ between rapamycin-and vehicle-treated animals. In contrast, peak rotation angle was significantly increased after rapamycin treatment. This effect was associated with a significantly decreased torsional stiffness. At 5 weeks post-fracture, no significant differences in torque, rotation angle and stiffness could be detected between rapamycin-treated animals and vehicle-treated controls (Table 1).

Histomorphometric analysis
The results of the histomorphometric analysis showed that callus size was found significantly decreased in rapamycin-treated animals at 2 weeks when compared with vehicle-treated controls. In addition, bone formation within the callus was reduced, whereas the fraction of cartilage and fibrous tissue was slightly increased after rapamycin treatment. It is interesting to note that the histomorphometric analyses further confirmed the radiological investigations, demonstrating that at 5 weeks post-fracture the size of the callus increased in the rapamycin group but decreased in the control group. At this time point cartilaginous and fibrous tissue had disappeared in almost all samples of both groups. Accordingly, callus was composed mainly of bone without significant differences between rapamycin-treated animals and vehicle-treated controls (Figures 2 and 3).

Immunohistochemical analysis
At 2 weeks post-fracture PCNA-positive staining was found in periosteal cells, endothelial cells and osteoblasts. For all cell types analyzed a reduced fraction of PCNA-positive cells was observed after rapamycin treatment when compared with vehicle-treated controls (periosteal cells: 2.0 ± 2.2 versus $12.0 \pm 4.0\%$; endothelial cells: 0.0 ± 0.0 versus $36.3 \pm 8.1\%$; osteoblasts: 2.1 ± 2.2 versus $27.0 \pm 4.0\%$) (Figure 4).

Staining for VEGF was found in hypertrophic chondrocytes at 2 weeks post-fracture. Interestingly, the quantitative analysis revealed a higher fraction of positive cells in vehicle-treated controls ($21.7 \pm 3.5\%$) compared with rapamycin-treated animals ($3.7 \pm 3.7\%$) (Figure 5).

Vascular density analysis
The quantitative analysis of area density of vessel profiles at the endochondral ossification front revealed a lower number of vessels in rapamycin-treated animals when compared with vehicle-treated controls (2 ± 4 versus $16 \pm 6 \, mm^{-2}$) (Figure 6).
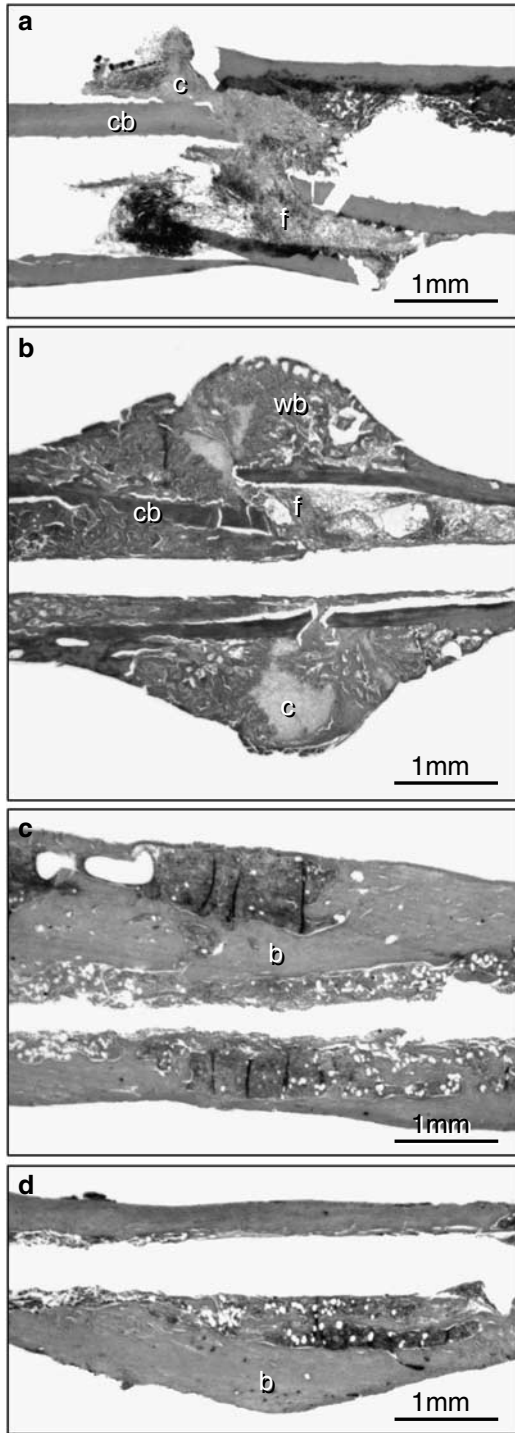
Western blot analysis
At 2 weeks, all samples showed characteristic bands according to the molecular weight of PCNA and VEGF, indicating cell proliferative action and angiogenesis. However, the western blotting analysis revealed a reduced expression of both PCNA and VEGF in rapamycin-treated animals when compared with vehicle-treated controls (Table 2 and Figure 7).

ELISA analysis
Consistent with the findings of the western blot analysis, ELISA analysis at 2 weeks revealed a higher expression of PCNA and VEGF in control animals when compared with rapamycin-treated animals (Table 3).

Discussion and conclusions

Rapamycin is a therapeutic immunosuppressant drug, widely used following organ transplantation (Wiederrecht *et al.*, 1995) and has been used as an anti-angiogenic drug for direct cancer treatment (Guba *et al.*, 2002). However, there is no information on whether rapamycin affects bone repair, although several studies have shown negative effects of rapamycin and other immunosuppressive drugs on bone development and metabolism (Romero *et al.*, 1995; Stempfle *et al.*, 2002; Compston, 2003; Vossen *et al.*, 2005; Alvarez-Garcia *et al.*, 2007). Therefore, this study was undertaken to analyze the effect of systemic rapamycin treatment on bone healing.

Figure 1 Radiological analysis of callus diameter in relation to the diameter of the femur at the fracture site, after rapamycin (RAPA) treatment. All data are given as mean ± s.d. *$P<0.05$ versus corresponding values of the vehicle-treated controls. #$P<0.05$ versus corresponding values of specimens at 2 weeks post-fracture.

Table 1 Biomechanical analysis of the callus of rapamycin (RAPA)-treated animals and vehicle-treated controls at 2 and 5 weeks post-fracture

	2 weeks			5 weeks		
	RAPA	*Control*	P	*RAPA*	*Control*	P
Peak torque [%]	22.3 ± 3.3	24.5 ± 5.6	0.65	62.6 ± 18.5	55.2 ± 12.2	0.39
Peak rotation angle [%]	254.3 ± 159.9	110.1 ± 55.1	0.05	51.8 ± 16.7	59.5 ± 14.3	0.37
Torsional stiffness [%]	11.5 ± 5.9	28.3 ± 13.9	0.02	142.3 ± 92.4	94.7 ± 15.5	0.21

Data are given as mean ± s.d. Peak torque, peak rotation angle and torsional stiffness of the fractured site are given in percent of the unfractured bone of the contralateral site.

Rapamycin affects fracture healing
JH Holstein *et al*
1059

Figure 2 Longitudinal sections of the callus of femora at 2 (**a** and **b**) and 5 (**c** and **d**) weeks of fracture healing stained according to the trichrome method. **a** and **c** show the callus of rapamycin-treated animals, **b** and **d** that of controls. At 2 weeks, callus consisted of cartilaginous (c) and fibrous (f) tissue as well as of cortical (cb) and newly woven bone (wb). Note that at 2 weeks callus is dominated by newly woven bone in the control animal (**b**), whereas callus formation is significantly diminished after rapamycin treatment (**a**). At 5 weeks post-fracture cartilaginous and fibrous tissue disappeared completely in both groups. A distinction between newly maturing bone (b) and old surrounding bone (b) is not evident.
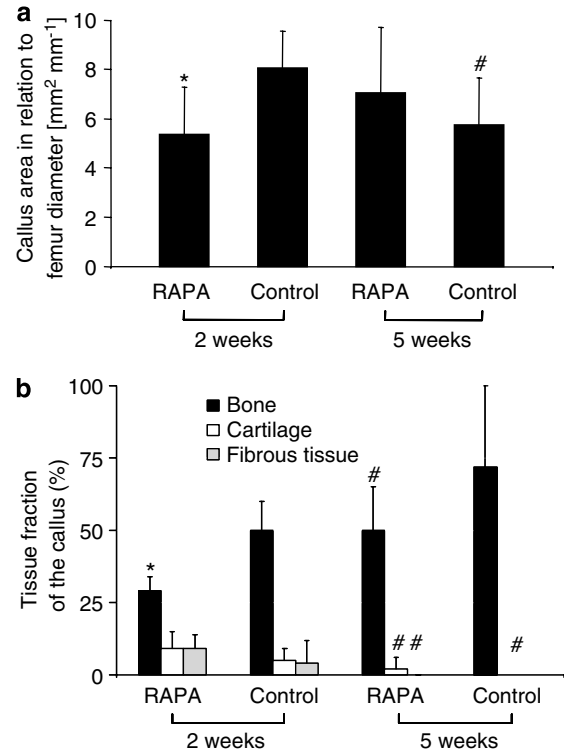

Figure 3 Histomorphometric analysis of (**a**) callus size in relation to the diameter of the femur at the fracture site and (**b**) composition of the different tissues within the callus in relation to the total callus (bone callus area (mineralized bone, osteoid and bone marrow) in relation to total callus area [B.Cl.Ar Cl.Ar^{-1}]; cartilaginous callus area in relation to total callus area [Cg.Cl.Ar Cl.Ar^{-1}]; fibrous callus area in relation to total callus area [Fb.Cl.Ar Cl.Ar^{-1}]). All data are given as means ± s.d. RAPA = rapamycin *$P< 0.05$ versus corresponding values of vehicle-treated controls. #$P<0.05$ versus corresponding values of specimens at 2 weeks post-fracture.

We demonstrated that rapamycin treatment leads to a severe alteration of early fracture healing, as indicated by a decreased torsional stiffness at 2 weeks post-fracture. This effect was associated with a significant inhibition of hard callus formation together with a dramatically reduced formation of new woven bone as measured by histomorphometric analysis.

Rapamycin has been suggested to possess strong anti-angiogenic activities linked to a decrease in production of VEGF (Guba *et al*., 2002; Laschke *et al*., 2006). In growth plates of young rats, Alvarez-Garcia *et al*. (2007) demonstrated that rapamycin reduces chondrocyte proliferation and maturation during endochondral ossification, which was associated with a decreased resorption of cartilage and an alteration of vascular invasion. Interestingly, this effect was linked to a decreased VEGF expression in hypertrophic chondrocytes after rapamycin treatment.

It is well known that VEGF is one of the key growth factors promoting endochondral ossification also during secondary fracture healing. This stage of fracture healing consists of (i) terminal chondrocyte differentiation and cell death, (ii) extracellular matrix degradation and calcification as well as (iii) angiogenesis and osteogenesis (Miclau and Helms, 2000). VEGF has been reported to be expressed in terminally differentiating chondrocytes,
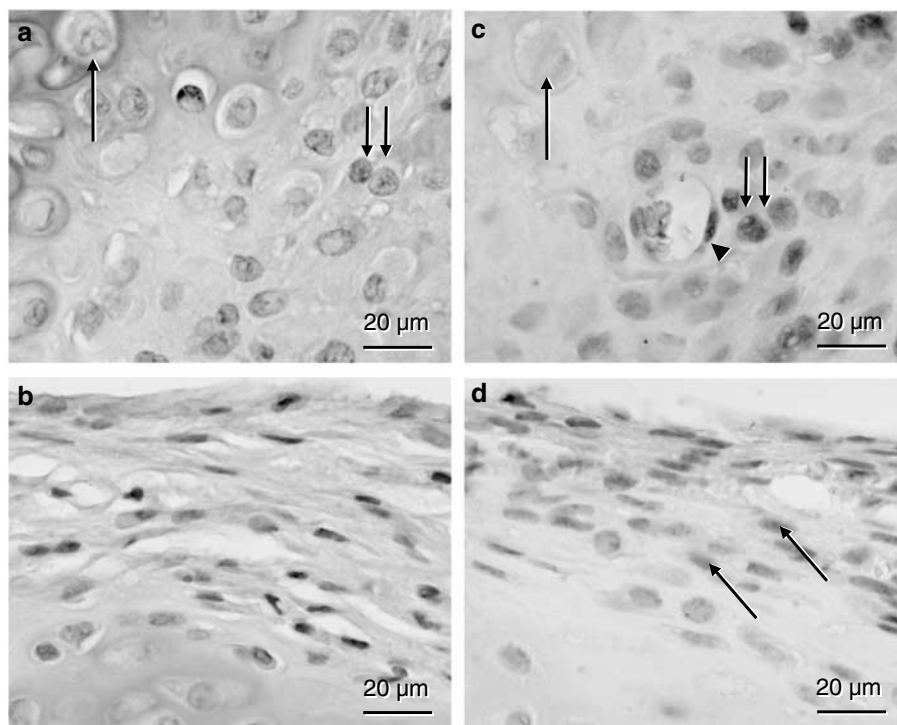
Figure 4 Immunohistochemistry of cell proliferation as indicated by proliferating cell nuclear antigen (PCNA) expression within the callus of a rapamycin-treated animal (**a** and **b**) and a control animal (**c** and **d**) at 2 weeks post-fracture. **a** and **c** represent the transition between the cartilaginous and the osseous fraction of the callus, where hypertrophic chondrocytes (arrow) are replaced by proliferating osteoblasts (double arrow). Note in the control animal the positive-stained osteoblasts, which follow invading vessel profiles containing PCNA positive endothelial cells (arrow head). In the periosteum (**b** and **d**), positive PCNA staining is found only in cells of the control (arrows) but not of the rapamycin-treated animal.

coincidently with the onset of vascularization and subsequent ossification of the callus (Ferguson *et al.*, 1999). Hence, the negative action of rapamycin on fracture repair at 2 weeks post-fracture might be due to an inhibition of VEGF expression in hypertrophic chondrocytes as shown by immunohistochemical analysis. This view is supported by the results of the western blot and ELISA analysis, demonstrating a reduced callus expression of VEGF after rapamycin treatment during the early phase of fracture healing. On the other hand, the decreased amount of VEGF expression might also be a consequence of altered cell proliferation and differentiation as indicated by the lower PCNA content in the callus of rapamycin-treated animals when compared with vehicle-treated controls. This effect, however, is rather unlikely, because VEGF is almost exclusively produced in chondrocytes and, as shown by immunohistochemistry, the hypertrophic chondrocytes did not show any PCNA staining, regardless whether the animals received rapamycin treatment or not.

Previously, we and other groups demonstrated, by immunohistochemical methods, intensive staining of PCNA in proliferating osteoblasts at 2 weeks post-fracture (Iwaki *et al.*, 1997; Holstein *et al.*, 2007b). Recent *in vitro* studies demonstrated that rapamycin affects osteoblast proliferation and the early stage of osteoblast differentiation (Isomoto *et al.*, 2007; Singha *et al.*, 2008).

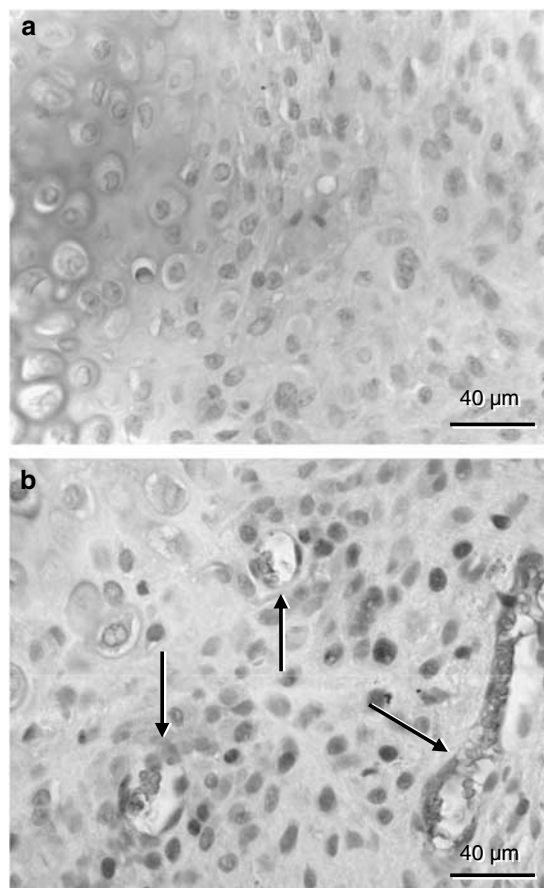During endochondral ossification VEGF couples hypertrophic chondrocyte differentiation and neovascularization of the endochondral ossification front, both of which play a critical role in the process of osteogenesis (Gerber *et al.*, 1999). Therefore, we suggest that the inhibition of neovascularization, as demonstrated by our morphometric analysis of vessel profiles and the decrease of bone formation might both be a consequence of VEGF inhibition through rapamycin treatment.

At 5 weeks the negative action of rapamycin on fracture healing was abolished. Late callus growth, morphological bone formation and biomechanical callus strength and stiffness were all similar to those measured at five weeks in vehicle-treated controls. These observations suggest that rapamycin delays initial fracture healing, but is not capable of completely preventing new bone formation. Accordingly, angiogenesis and vascularization, most probably inhibited through the suppression of VEGF by rapamycin, have to be considered to play a substantial role for accelerating the process of fracture healing.

Although the anti-angiogenic properties of rapamycin are supposed to be mediated by the inhibition of VEGF (Guba *et al.*, 2002), the immunosuppressive action of rapamycin is based on a reduction of interleukin-2-stimulated T-cell division (Wiederrecht *et al.*, 1995). Interestingly, T-cells have been shown to be absent in areas of new woven bone, whereas T-cells can be found in abundance within the fibrous fraction of the callus (Andrew *et al.*, 1994). Also, CD4-positive T-cells are proposed to be the predominant inflammatory cell responsible for delayed fracture healing and these cells are notably absent during active bone formation (Santavirta *et al.*, 1992; Andrew *et al.*, 1994). These findings
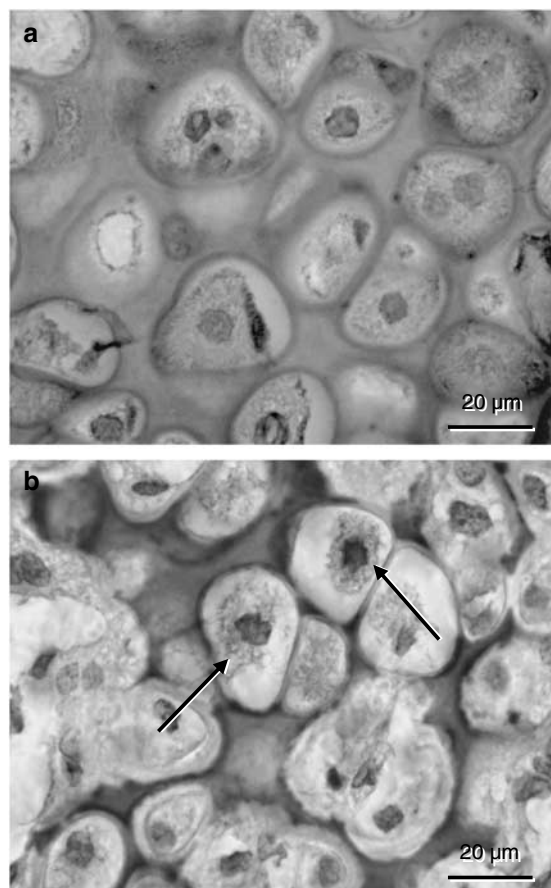
Figure 5 Immunohistochemistry of vascular endothelial growth factor (VEGF) expression within the callus of a rapamycin-treated (**a**) and a control animal (**b**) at 2 weeks post-fracture. In contrast to the rapamycin-treated animal, several hypertrophic chondrocytes of the control animal show positive staining for VEGF in the cytoplasm (arrows).
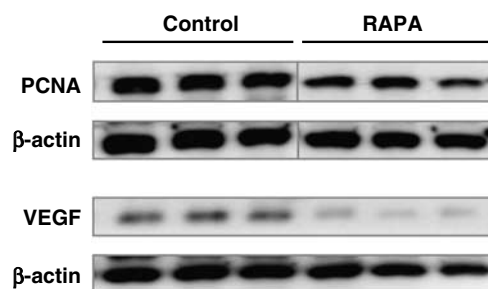
Table 2 Western blot analysis of PCNA and VEGF expression in callus of rapamycin (RAPA)-treated animals and vehicle-treated controls at 2 weeks post-fracture

| | 2 weeks | |
	RAPA	*Control*
PCNA [OD mm^2]	9.2 ± 2.6	16.3 ± 2.3
VEGF [OD mm^2]	5.7 ± 1.3	13.7 ± 1.8

Data are given as mean $\pm$ s.d.

might explain the increase of bone formation in the rapamycin-treated animals during the later phase of the 5-week healing period. During this phase rapamycin might contribute to the replacement of the fibrous tissue within the callus by new woven bone. Overall, the negative action of rapamycin on fracture healing due to the inhibition of VEGF at 2 weeks may be counteracted at 5 weeks by an acceleration of bone formation due to T-cell suppression.

Interestingly, other widely used immunosuppressive drugs such as cyclosporin A (CsA) and FK506 (tacrolimus) do not influence fracture healing in the experimental setting (Warren *et al.*, 1985; Voggenreiter *et al.*, 2005). These

Figure 6 Vessel profiles at the transition between hypertrophic cartilage and woven bone in proliferating cell nuclear antigen (PCNA)-stained sections at 2 weeks post-fracture. In contrast to the rapamycin-treated animal (**a**), several vessels (arrows) are found in the vehicle-treated control (**b**).

Figure 7 Western blot analysis of proliferating cell nuclear antigen (PCNA) and vascular endothelial growth factor (VEGF) expression within the callus after 2 weeks of fracture healing. Note the reduced expression of PCNA and VEGF in rapamycin (RAPA)-treated animals when compared with that of vehicle-treated controls. β-actin was used as loading control.

observations are probably due to the fact that the mechanism of immunosuppression differs between CsA and FK506, which represent calcineurin inhibitors and rapamycin, which is an inhibitor of mTOR (Schmelzle and Hall, 2000).

To conclude, we demonstrate in the present study that rapamycin affects early fracture healing, most probably by an inhibition of cell proliferation and neovascularization associated with a decreased VEGF expression in hypertrophic

Table 3 ELISA analysis of PCNA and VEGF expression in callus of rapamycin (RAPA)-treated animals and vehicle-treated controls at 2 weeks post-fracture

	2 weeks	
	RAPA	*Control*
PCNA [pg ml^{-1}]	40 ± 23	380 ± 95
VEGF [pg ml^{-1}]	49 ± 19	126 ± 16

Data are given as mean $\pm$ s.d.

chondrocytes. Considering the increasing administration of rapamycin in transplant and cancer patients, the potential detrimental effects of rapamycin should be kept in mind when treating patients with bone fractures.

Acknowledgements

Conflict of interest

The authors state no conflict of interest.

References

Alvarez-Garcia O, Carbajo-Perez E, Garcia E, Gil H, Molinos I, Rodriguez J *et al.* (2007). Rapamycin retards growth and causes marked alterations in the growth plate of young rats. *Pediatr Nephrol* **7**: 954–961.

Andrew JG, Andrew SM, Freemont AJ, Marsh DR (1994). Inflammatory cells in normal human fracture healing. *Acta Orthop Scand* **65**: 462–466.

Compston JE (2003). Osteoporosis after liver transplantation. *Liver Transpl* **9**: 321–330.

Cross SE, Richards SK, Clark A, Benest AV, Bates DO, Mathieson PW *et al.* (2007). Vascular endothelial growth factor as a survival factor for human islets: effect of immunosuppressive drugs. *Diabetologia* **50**: 1423–1432.

Ferguson C, Alpern E, Miclau T, Helms JA (1999). Does adult fracture repair recapitulate embryonic skeletal formation? *Mech Dev* **87**: 57–66.

Geiger F, Bertram H, Berger I, Lorenz H, Wall O, Eckhardt C *et al.* (2005). Vascular endothelial growth factor gene-activated matrix (VEGF(165)-GAM) enhances osteogenesis and angiogenesis in large segmental bone defects. *J Bone Miner Res* **20**: 2028–2035.

Gerber HP, Vu TH, Ryan AM, Kowalski J, Werb Z, Ferrara N (1999). VEGF couples hypertrophic cartilage remodeling, ossification and angiogenesis during endochondral bone formation. *Nat Med* **5**: 623–628.

Guba M, von Breitenbuch P, Steinbauer M, Koehl G, Flegel S, Hornung M *et al.* (2002). Rapamycin inhibits primary and metastatic tumor growth by antiangiogenesis: involvement of vascular endothelial growth factor. *Nat Med* **8**: 128–135.

Holstein JH, Menger MD, Meier C, Culemann U, Pohlemann T (2007a). Development of a locking femur nail for mice. *J Biomech* **40**: 215–219.

Holstein JH, Menger MD, Scheuer C, Meier C, Culemann U, Wirbel RJ *et al.* (2007b). Erythropoietin (EPO)—EPO-receptor signalling improves early endochondral ossification and mechanical strength in fracture healing. *Life Sci* **80**: 893–900.

Isomoto S, Hattori K, Ohgushi H, Nakajima H, Tanaka Y, Takakura Y (2007). Rapamycin as an inhibitor of osteogenic differentiation in bone marrow-derived mesenchymal stem cells. *J Orthop Sci* **1**: 83–88.

Iwaki A, Jingushi S, Oda Y, Izumi T, Shida JI, Tsuneyoshi M *et al.* (1997). Localization and quantification of proliferating cells during rat fracture repair: detection of proliferating cell nuclear antigen by immunohistochemistry. *J Bone Miner Res* **12**: 96–102.

Kauffman HM, Cherikh WS, McBride MA, Cheng Y, Hanto DW (2006). Post-transplant *de novo* malignancies in renal transplant recipients: the past and present. *Transpl Int* **19**: 607–620.

Laschke MW, Elitzsch A, Scheuer C, Holstein JH, Vollmar B, Menger MD (2006). Rapamycin induces regression of endometriotic lesions by inhibiting neovascularization and cell proliferation. *Br J Pharmacol* **149**: 137–144.

MacDonald A, Scarola J, Burke JT, Zimmerman JJ (2000). Clinical pharmacokinetics and therapeutic drug monitoring of sirolimus. *Clin Ther* **22S**: B101–B121.

Miclau T, Helms JA (2000). Molecular aspects of fracture healing. *Curr Opin Orthop* **11**: 367–371.

Müller ME, Nazarian S, Koch P, Schatzker J (1990). *The Comprehensive Classification of Fractures of Long Bones*. Springer-Verlag: Heidelberg New York.

Navasa M, Forns X, Sanchez V, Andreu H, Marcos V, Borras JM *et al.* (1996). Quality of life, major medical complications and hospital service utilization in patients with primary cirrhosis after liver transplantation. *J Hepatol* **25**: 129–134.

Neufeld G, Cohen T, Gengrinovitch S, Poltorak Z (1999). Vascular endothelial growth factor (VEGF) and its receptors. *FASEB J* **13**: 9–23.

Parfitt AM, Drezner MK, Glorieux FH, Kanis JA, Malluche H, Meunier PJ *et al.* (1987). Bone histomorphometry: standardization of nomenclature, symbols, and units. Report of the ASBMR Histomorphometry Nomenclature Committee. *J Bone Miner Res* **2**: 595–610.

Romero DF, Buchinsky FJ, Rucinski B, Cvetkovic M, Bryer HP, Liang XG *et al.* (1995). Rapamycin: a bone sparing immunosuppressant? *J Bone Miner Res* **10**: 760–768.

Santavirta S, Konttinen YT, Nordstrom D, Makela A, Sorsa T, Hukkanen M *et al.* (1992). Immunologic studies of nonunited fractures. *Acta Orthop Scand* **63**: 579–586.

Schaffer M, Schier R, Napirei M, Michalski S, Traska T, Viebahn R (2007). Sirolimus impairs wound healing. *Langenbecks Arch Surg* **392**: 297–303.

Schmelzle T, Hall MN (2000). TOR, a central controller of cell growth. *Cell* **103**: 253–262.

Singha UK, Jiang Y, Yu S, Luo M, Lu Y, Zhang J *et al.* (2008). Rapamycin inhibits osteoblast proliferation and differentiation in MC3T3-E1 cells and primary mouse bone marrow stromal cells. *J Cell Biochem* **103**: 434–446.

Stempfle HU, Werner C, Siebert U, Assum T, Wehr U, Rambeck WA *et al.* (2002). The role of tacrolimus (FK506)-based immunosuppression on bone mineral density and bone turnover after cardiac transplantation: a prospective, longitudinal, randomized, double-blind trial with calcitriol. *Transplantation* **73**: 547–552.

Voggenreiter G, Siozos P, Hunkemoller E, Heute S, Schwarz M, Obertacke U (2005). Immunosuppression with FK506 has no influence on fracture healing in the rat. *Bone* **37**: 227–233.

Vossen M, Edelstein J, Majzoub RK, Maldonado C, Perez-Abadia G, Voor MJ *et al.* (2005). Bone quality and healing in a swine vascularized bone allotransplantation model using cyclosporine-based immunosuppression therapy. *Plast Reconstr Surg* **115**: 529–538.

Wallemacq PE, Vanbinst R, Asta S, Cooper DP (2003). High-throughput liquid chromatography-tandem mass spectrometric analysis of sirolimus in whole blood. *Clin Chem Lab Med* **41**: 921–925.

Warren SB, Pelker RR, Friedlaender GE (1985). Effects of short-term cyclosporin-A on biomechanical properties of intact and fractured bone in the rat. *J Orthop Res* **3**: 96–100.

Wiederrecht GJ, Sabers CJ, Brunn GJ, Martin MM, Dumont FJ, Abraham RT (1995). Mechanism of action of rapamycin: new insights into the regulation of G1-phase progression in eukaryotic cells. *Prog Cell Cycle Res* **1**: 53–71.